Backwater effect due to a single spur dike

Article *in* Canadian Journal of Civil Engineering · February 2011

DOI: 10.1139/l06-117

2 authors, including:

James A Kells
University of Saskatchewan
39 PUBLICATIONS **715** CITATIONS

Backwater effect due to a single spur dike

H. Azinfar and J.A. Kells

Abstract: Spur dikes are river engineering structures that project from the bank of a stream at some angle to the main flow direction. They are principally used for river training and protection of the riverbank from erosion. A spur dike might be considered a form of macroscale boundary roughness, which produces a backwater effect upstream from the spur dike location. Despite this impact, spur dike design often proceeds without regard to the effect that the spur dike might have on the stream system. The work presented herein is on the backwater effect due to a single, vertical-walled spur dike. It is based on a momentum analysis in which the resistance offered by the spur dike is represented by a drag equation, for which the key parameter is the spur dike drag coefficient. Experimental data acquired for various configurations of a single spur dike within fixed-bed flumes have been used to calibrate and validate the proposed backwater model. The results show that the spur dike drag coefficient, hence the computed backwater effect, depends on the channel contraction caused by the spur dike, the degree of spur dike submergence, the aspect ratio of the spur dike, and the Froude number of the flow.

Key words: spur dike, backwater effect, physical model, momentum principle, drag force, drag coefficient, river engineering.

Résumé : Les épis sont des structures potamotechniques qui font saillie des berges d'un ruisseau à un certain angle par rapport à la direction principale de l'écoulement. Ils sont principalement utilisés pour la correction d'un cours d'eau et la protection des rives contre l'érosion. Un épi peut être considéré comme étant une forme de rugosité limite à grande échelle, qui produit un effet de remous en amont de l'épi. Malgré cet impact, la conception des épis ne tient souvent pas compte de l'effet que pourrait avoir l'épi sur le cours d'eau. Cet article présente l'effet de remous causé par un seul épi à murs verticaux. Il est basé sur une analyse du mouvement dans laquelle la résistance présentée par l'épi est représentée par une équation de traînée, dans laquelle le paramètre clé est le coefficient de traînée de l'épi. Les données expérimentales acquises pour diverses configurations d'un seul épi dans les canaux sur appui à lit fixe ont été utilisées pour étalonner et valider le modèle de remous proposé. Les résultats montrent que le coefficient de traînée de l'épi, et donc l'effet de remous calculé, est déterminé par la contraction du chenal engendrée par l'épi, le niveau de submersion de l'épi, le rapport de forme de l'épi et le nombre de Froude de l'écoulement.

Mots-clés : épi, effet de remous, modèle physique, principe de mouvement, force de traînée, coefficient de traînée, potamotechnie.

[Traduit par la Rédaction]

1. Introduction

Spur dikes are hydraulic structures that project from the bank of a stream at some angle to the main flow direction. They are principally used for two purposes, namely river training and erosion protection of a riverbank. River training applications of spur dikes frequently involve improving the navigability of a river by increasing the flow depth, straightening the channel alignment, and increasing the sediment transport rate through the improved reach. The latter feature results in reduced costs for channel dredging. In the case of bank protection, spur dikes deflect the flow away from the bank, thereby reducing the near-bank flow velocity and often creating a region of deposition. Relative to other approaches, such as revetments, spur dikes are among the most economical structures that can be used for riverbank protection (Shields 1995). Despite their useful features, however, there is some concern that spur dikes may be responsible for increased flooding due to the associated backwater effect. For example, studies show that, over the past century, flood stages for given discharges at various locations along the Middle Mississippi and Lower Missouri rivers have increased by 2–4 m (Criss and Shock 2001). These river reaches are characterized by extensive river engineering works, including spur dikes and levees. Pinter (2004) confirms the reported increase in flood stage due to the presence of engineering works on the two rivers.

The relative increase in a river's stage and attendant flooding can be due to a modified hydrologic regime, changes in the hydraulic regime, or both. To separate the effects of the two factors, Criss and Shock (2001) and Pinter et al. (2001) tracked the changes in the Mississippi and Missouri river stages over time for constant-discharge conditions. With the discharge being held constant, the variations in a river's stage can be attributed solely to changes in the channel hy-

Received 14 July 2005. Revision accepted 8 August 2006. Published on the NRC Research Press Web site at http://cjce.nrc.ca on 9 March 2007.

H. Azinfar and J.A. Kells.[1] Department of Civil and Geological Engineering, University of Saskatchewan, 57 Campus Drive, Saskatoon, SK S7N 5A9, Canada.

Written discussion of this article is welcomed and will be received by the Editor until 31 May 2007.

[1]Corresponding author (e-mail: Jim.Kells@usask.ca).

 doi:10.1139/L06-117

draulics, and the effects of a modified hydrologic regime are eliminated. Based on their analysis, Criss and Shock and Pinter et al. observed that the relative stages of the Mississippi and Missouri rivers have increased over the last century. These findings suggest that the channel roughness of the rivers has increased, which the researchers attribute to the construction of river engineering works such as spur dikes. They also observed that the increase in channel roughness is more important for higher discharge conditions. At low discharges, in the case of an erodible boundary channel, there may even be a decrease in the river's stage, which can be attributed to main channel degradation due to channel confinement resulting from spur dike construction. As well, many rivers with river engineering works, such as the Mississippi River, contain both spur dikes and levees. Since levees are usually built to levels higher than the bankfull stage, Pinter et al. also concluded, for such rivers, that observed stage increases for flows less than bankfull can be attributed solely to spur dikes.

Stage increases due to spur dikes have also been reported on other rivers. For the Rhine River in Europe, for example, the height of the spur dikes was reduced as a way of reducing their adverse effects during times of flooding (Belz et al. 2001; Yossef 2002). Similarly, in a numerical study of the Nile River in Egypt, it was concluded that the construction of spur dikes has had a considerable effect on upstream water levels (Soliman et al. 1997). These increases in flood stage often endanger buildings, infrastructure (roadways, cables, bridges, etc.), farmland, hydraulic structures (pump stations, intakes, etc.), and people who live near the river.

Since it has now been demonstrated that the construction of spur dikes can significantly increase the stage of a river, especially during times of flooding, it is then prudent to quantify the amount of backwater effect that occurs so that the impacts of spur dike construction can be determined by those charged with managing the river system. For this reason, a study on the backwater effects associated with spur dikes was recently initiated at the University of Saskatchewan. The purpose of the study was to explore the various parameters that affect the resistance characteristics of spur dikes in open channels and to develop a model for quantifying the amount of backwater effect experienced. The work reported herein, which is part of a larger study on the backwater effect due to spur dikes, was based on a single spur dike having a basic geometric configuration (i.e., rectangular flat plates arranged perpendicular to the channel wall). In this paper, a theoretical framework based on the momentum principle is developed as a way of relating the backwater effect to the drag force exerted by a single spur dike, wherein the spur dike drag force is represented by a drag coefficient. Using the results from two physical models, experimental data acquired for various dimensions of a single spur dike within fixed-bed flumes have been used to calibrate and validate the proposed spur dike backwater model.

2. Theoretical framework

Any obstacle located within a flow field exerts a drag force on the flow, which invariably results in some type of energy loss. In free surface flow, such as the flow in a river, the energy loss is overcome by a rise in the upstream water level, herein termed the backwater effect. For nonstreamlined objects or bluff bodies, the approach flow separates from the boundaries of the object, producing a wake zone behind the object, which is characterized by eddies and a high rate of energy dissipation. The resulting difference in pressure from the upstream side of the object to the downstream side results in a net upstream force being exerted by the object on the flow. This force is known as form drag. In addition to form drag, there is often a small amount of drag resulting from the increased shear stress associated with the relatively high velocity flow over the surface of the object. This latter drag is called viscous drag or skin friction drag. The total drag force is the sum of the two types of drag. For bluff bodies, form drag is typically dominant. As spur dikes can be classified as bluff bodies, the drag resulting from a spur dike is primarily due to form drag. This drag is principally responsible for the energy loss and backwater effect at a spur dike.

The analysis of the backwater effect due to a spur dike in an open channel can be done using either an energy approach or a momentum approach. A momentum approach has been used in this work. With reference to Fig. 1, the one-dimensional linear momentum equation can be written between section 1 upstream of the spur dike and section 2 downstream to give

$$[1] \qquad F_1 - F_2 - F_D - F_f = \rho Q(\beta_2 V_2 - \beta_1 V_1)$$

where F_1 is the force due to the upstream hydrostatic pressure distribution; F_2 is the force due to the downstream hydrostatic pressure distribution; F_D is the drag force due to the spur dike; F_f is the friction force due to boundary friction between sections 1 and 2; ρ is the fluid density; Q is the discharge; V_1 and V_2 are the average velocities at sections 1 and 2, respectively; and β_1 and β_2 are the momentum correction factors applicable at sections 1 and 2, respectively. In this analysis, the channel is horizontal and thus there are no effects due to bed slope to be considered.

For this analysis, it is assumed that the friction force is negligible and that the momentum correction factors are equal to unity. These assumptions are common with many types of momentum analyses, and the impacts are often compensatory in nature (i.e., the effects of the two assumptions tend to offset each other), such as in the case of the hydraulic jump, although in this instance the impacts are additive. It might further be noted that, if the channel bed had a slope and the flow was uniform, the downstream component of the weight of the fluid within the control volume (i.e., between sections 1 and 2) would exactly offset the frictional resistance at the boundary. The drag force, F_D, can be expressed as

$$[2] \qquad F_D = C_D A_s \rho V^2/2$$

where C_D is the drag coefficient, and A_s is the upstream projected area of the spur dike (i.e., $A_s = PL$, where P is the height of the spur dike and L is the length of the spur dike perpendicular to the flow). The velocity, V, is a representative velocity, which for this work has been taken to be the approach velocity, V_1. On this basis, eq. [1] can be revised to read

$$[3] \qquad \rho g B h_1^2/2 - \rho g B h_2^2/2 - C_D A_s \rho V_1^2/2 = \rho Q(V_2 - V_1)$$

Fig. 1. Schematic (plan and profile) of a spur dike within a control volume. Numbers 1 and 2 are sections referred to in the text. ▽, water surface.

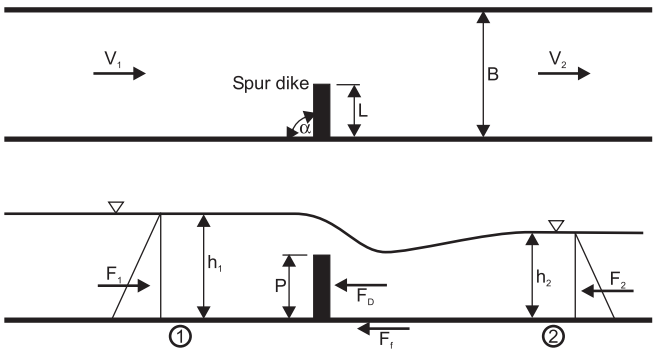

where the hydrostatic pressure force terms have been expressed in terms of the flow depth; B is the channel width; g is the acceleration due to gravity (i.e., 9.81 m/s^2); and h_1 and h_2 are the upstream and downstream flow depths, respectively. The backwater effect, which is the subject of this investigation, is represented by the difference between the upstream and downstream flow depths (i.e., $h_1 - h_2$).

Further manipulation of eq. [3] in conjunction with the continuity equation leads to

$$[4] \quad 2Fr_1^2(h_1/h_2)^3 - (2Fr_1^2 - C_D A_r Fr_1^2 + 1)(h_1/h_2)^2 + 1 = 0$$

where the area ratio, A_r, is given by A_s/Bh_1; and Fr_1 is the Froude number of the approach flow. If the tailwater conditions, spur dike geometry, and drag coefficient are known, eq. [4] can be solved implicitly for h_1/h_2 to obtain the upstream water depth and the corresponding backwater effect resulting from the spur dike. If Newton's method is used in the solution procedure, the first derivative of eq. [4] is required, which is given by

$$[5] \quad f'(h_1/h_2) = 2(h_1/h_2)(Fr_1^2 - C_D A_r Fr_1^2 - 1)$$

Even so, the key issue requiring resolution at this stage is the determination of the spur dike drag coefficient.

From dimensional analysis, the drag coefficient can be expressed in terms of a functional equation as

$$[6] \quad C_D = f_a(Re_1,\ Fr_1,\ L/B,\ P/L,\ h_1/P,\ \Delta,\ \alpha)$$

where Re_1 is the Reynolds number of the approach flow, L/B is the spur dike contraction ratio, P/L is the spur dike aspect ratio, h_1/P is the spur dike submergence ratio, Δ is the spur dike shape factor, and α is the angle between the spur dike and the stream bank as measured from upstream. The Reynolds number represents the effects of viscosity, which are assumed to be insignificant in the case of a flow field involving a spur dike. Moreover, since only a vertical-walled spur dike is considered in this study, the spur dike shape factor can be omitted from the analysis. Similarly, only one spur dike orientation was used in this work, with the spur dike being oriented normal to the stream bank (i.e., $\alpha = 90°$). Thus, for this work, the spur dike drag coefficient can be expressed by a simplified functional equation as

$$[7] \quad C_D = f_b(Fr_1,\ L/B,\ P/L,\ h_1/P)$$

In turn, eq. [7] can be expressed in a more useful mathematical form as

$$[8] \quad C_D = K(P/L)^a\,(1 - L/B)^b\,(h_1/P)^c\,(Fr_1)^d$$

where K, a, b, c, and d are assumed to be constants, which must be determined by experiment. In this work, the drag coefficient in eq. [8] has been expressed using values representative of the upstream flow conditions.

A parameter referred to as the opening ratio, defined herein as $1 - L/B$, has been used instead of the contraction ratio, L/B, in eq. [8]. Using the opening ratio avoids the problem of the drag coefficient approaching zero as the contraction ratio approaches zero. Thus, as the opening ratio approaches unity (i.e., there is little to no contraction of the channel due to the spur dike), the contraction ratio approaches zero, which means that there is negligible effect of the parameter on the computed drag coefficient, as is to be expected.

3. Experiments and model development

The data obtained from a series of experiments carried out by Oak (1992) have been used to calibrate eq. [8]. An 800 mm wide, horizontal, fixed-bed flume containing smooth, blunt end (i.e., rectangular), vertical-walled spur dikes of various lengths and heights was used in Oak's work. The test conditions included evaluation of both submerged and unsubmerged spur dikes. Table 1 shows the range of parameters studied by Oak.

In addition to the aforementioned experiments for vertical-walled spur dikes, Oak (1992) also conducted experiments for spur dikes having a triangular cross section and a rounded nose and both smooth and rough boundaries. These latter spur dikes were also tested for both submerged and unsubmerged modes of operation. However, only the data for Oak's smooth, blunt end, vertical-walled, submerged spur dikes have been considered in this study. In this regard, two points are worth noting. First, the most critical condition with respect to the backwater effect due to a spur dike is for flood conditions, during which time the spur dike is likely to be submerged. Second, as found by Oak and Smith (1994), the backwater effect associated with a spur dike having a triangular cross section and a rounded nose is less than that for a spur dike having a blunt end and vertical orientation. The streamlining associated with the former geometry results in a reduced backwater effect. As such, the results of the work reported herein can be considered to be somewhat conservative with respect to the predicted backwater effect.

In Oak's (1992) experiments, both the upstream and downstream water levels were measured for each of several spur dike geometries and flow conditions. Thus, it is possible to reanalyze Oak's data using eq. [3] expressed in terms of the drag coefficient as

$$[9] \quad C_D = \frac{2q^2(1/h_1 - 1/h_2) + g(h_1^2 - h_2^2)}{(A_s/B)(q/h_1)^2}$$

where q is the unit discharge (i.e., Q/B). Using eq. [9] to determine the drag coefficient for 540 tests from Oak's work and applying multiple variable regression analysis to the dataset for an equation expressed in the form of eq. [8] resulted in

Table 1. Range of experimental parameters used in Oak's (1992) experiments.

Spur dike height, P (mm)	100, 150, 200
Spur dike length, L (mm)	320, 400, 480
Channel width, B (mm)	800
Channel slope, S_o (m/m)	0
Downstream depth, h_2 (mm)	100–254
Downstream Froude number, Fr_2	0.05–0.40
Submergence ratio, h_1/P	1.03–1.77
Discharge, Q (L/s)	13.9–42.3

$$[10] \quad C_D = 4.00(P/L)^{-0.431}(1 - L/B)^{-0.849} \times (h_1/P)^{-1.676}(Fr_1)^{-0.221}$$

The software SPSS (Statistical Package for the Social Sciences, version 9; SPSS Inc. 1999) was used for this analysis. The resulting value of R^2, where R is the correlation coefficient, was found to be 0.88. In this work, the combination of eqs. [4] and [10] is referred to as the regression backwater model.

On the basis of the exponent values given in eq. [10], it is evident that the submergence ratio has the greatest effect on the drag coefficient (i.e., largest exponent) while the Froude number has the least effect (i.e., smallest exponent). In doing the analysis for eq. [10], at least three of the parameters used to describe the drag coefficient are physically independent, including the aspect ratio, P/L, the opening ratio, $1 - L/B$, and the submergence ratio, h_1/P. It was suspected, however, that there may be a relationship between the submergence ratio, h_1/P, and the Froude number, Fr_1, given that both variables depend on the flow rate, but covariance analysis using SPSS applied to Oak's (1992) data showed that there is no significant relationship between the two variables. Thus, on the basis of variable independence, it is possible to define the drag coefficient as

$$[11] \quad C_D = \varphi_1 \varphi_2 \varphi_3 \varphi_4$$

where the various φ terms, which are each a type of drag coefficient, can be defined as

$$[12] \quad \varphi_1 = f_1(P/L), \quad \varphi_2 = f_2(1 - L/B) \quad \varphi_3 = f_3(h_1/P), \quad \varphi_4 = f_4(Fr_1)$$

Equations [4] and [11] are referred to herein as the multiple function backwater model. This model is discussed further in the following paragraphs.

To develop the various φ relationships described in eq. [12], recourse was again made to Oak's (1992) data and the results of the multiple variable regression analysis expressed by eq. [10]. In doing this, each φ term was individually evaluated by dividing the computed drag coefficient by all of the remaining parameters in eq. [10], one by one. For example, in the case of φ_1, which represents the aspect ratio term in eq. [10] (i.e., the P/L term), the data were expressed as

$$[13] \quad \varphi_1 = \frac{C_D}{4.00(1 - L/B)^{-0.849}(h_1/P)^{-1.676}(Fr_1)^{-0.221}}$$

The same procedure was applied to all other φ terms. Equation [13] in essence reveals the nature of the variation of the drag coefficient with the aspect ratio, P/L, as the effects of the other variables have essentially been factored out. In this way, comparison can be made to the literature in respect of this parameter (and, in turn, the other three parameters too). As well, it is also possible to gain some insight to the physics of the problem, largely because the analysis procedure allows one parameter to be evaluated at a time.

The results of the analysis described previously, which quantifies the functional relationships expressed by eq. [12], are shown in Fig. 2. In each of the four plots in Fig. 2, it may be noted that the graphical relationship has been expressed in three ways: by a simple plot of the data (data points), by a power law least squares regression fit to the data (solid line), and by a curve fitted to an extended range of the data (broken line). In the case of the curve fitted to an extended range of the data, recourse was made to a review of the trend expressed by Oak's (1992) data, by applying simple logic to the basic physics of the problem (e.g., recognition of the physical limits of applicability), and by comparison with the results of related work in the published literature. The specific details applicable to each of the four φ parameters are discussed as follows.

Figure 2*a* shows the variation of φ_1 with the spur dike aspect ratio, P/L. Also included in this figure is the relationship for the drag coefficient of a rectangular flat plate positioned within a free-stream flow as given by Hoerner (1965). The upper range of the parameter φ_1 has been extended to lower values of P/L based on the trend expressed by Oak's data, and its lower range has been limited to a value of 1.2 on the basis of both the trend expressed by Oak's data and the drag coefficient of a rectangular flat plate for large aspect ratios as given by Hoerner. The resulting relationship for φ_1 as a function of P/L can then be expressed by

$$[14] \quad \varphi_1 = 1.8(1 - P/L)^{3.7} + 1.2$$

As indicated in Fig. 2*a*, except for aspect ratios greater than about 0.6, the experimental results for the drag coefficient from this study are greater than those for a rectangular plate located within a free-stream flow. It is postulated that the difference can be explained by the limited "ventilation" of the flow around the plate in the case of a spur dike, which is fastened to both the bed and one sidewall, versus the free-stream situation in which flow can access the backside of the plate from all sides. This explanation is supported by the work of Ranga Raju et al. (1983), who measured the drag coefficient of circular cylinders in an open channel. In that work, it was observed that the drag coefficient for a circular cylinder fastened to the floor of a flume is greater than that for the case of the same cylinder located within a free-stream environment. Dalton and Masch (1968) made a similar observation. In their case, Dalton and Masch argued that the horseshoe vortex near the flume bottom increases the stagnation pressure in front of the cylinder, which in turn results in an increase in the drag coefficient.

Figure 2*b* shows the variation of φ_2 with the spur dike opening ratio, $1 - L/B$. A power law equation has been used to describe the φ_2 relationship, as with eq. [10], viz.

$$[15] \quad \varphi_2 = (1 - L/B)^{-0.85}$$

Fig. 2. Contribution of the various parameters to the drag coefficient: (*a*) spur dike aspect ratio, *P*/*L*; (*b*) spur dike opening ratio, 1 – *L*/*B*; (*c*) spur dike submergence ratio, h_1/P; (*d*) upstream Froude number, Fr_1.

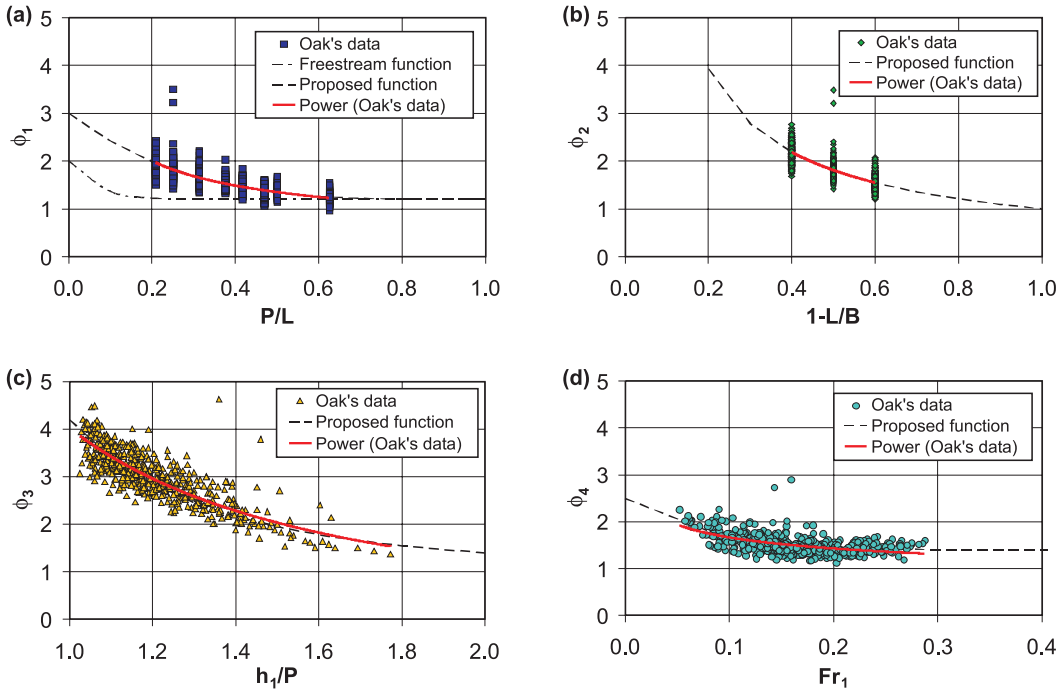

Two observations are readily apparent with eq. [15] and as shown in Fig. 2*b*. First, in the limit as *L*/*B* approaches zero, which means that there is no spur dike present, the value of φ_2 approaches unity. In essence, this means that there is no effect of the opening ratio on the drag coefficient for this situation, as expected. Second, the trend in the relationship is such that the drag coefficient increases with a decrease in the opening ratio (i.e., an increase in the contraction ratio). A similar finding was also made by Shaw (1971), who investigated the wall effect on the drag coefficient of a flat plate located within a water tunnel. Shaw noticed that, as the plate projected farther into the tunnel, the velocity at the point of flow separation increased, which in turn resulted in a decrease in the pressure on the leeward side of the plate. The decrease in pressure manifested itself as an increase in the drag coefficient, which Shaw found could be expressed using a power law function in terms of the opening ratio. Similarly, Ranga Raju et al. (1983) suggested the following power law function for circular cylinders located on the bed of a channel, viz.:

$$[16] \quad C_D = C_{Do}(1 - D/B)^{-1.35}$$

where C_D is the drag coefficient with contraction effects included, C_{Do} is the drag coefficient corresponding to a free-stream condition, *D* is the cylinder diameter, and *B* is the channel width. It is apparent that the form of eqs. [15] and [16] is essentially the same, with the only difference being the value of the exponent.

Figure 2*c* shows the variation of φ_3 with the submergence ratio, h_1/P. It can be seen that the drag coefficient decreases as the submergence ratio increases. This variation is attributed to the existence of the free surface flow. As the submergence ratio, hence water depth, increases, the effects of the free surface on the pressure difference between the upstream and downstream faces of the object decrease. The upper range of this parameter has been extended on the basis of the trend reflected in the data. The lower range has been extended both on the basis of the trend expressed by the data and by logic related to the physics of the problem. With respect to the latter point, it has been assumed that the value of φ_3 should approach unity (i.e., no effect due to submergence) as the submergence ratio approaches infinity. As such, the φ_3 relationship can be expressed as

$$[17] \quad \varphi_3 = \frac{3.2}{(h_1/P)^3} + 1$$

Malavasi and Guadagnini (2003) observed that the drag coefficient for rectangular bridge decks increases as the flow depth increases for submergence ratios less than one and decreases as the submergence ratio becomes greater than one. The maximum drag coefficient occurs for a submergence ratio near to unity. In their work, Malavasi and Guadagnini defined submergence ratio as the water depth above the bottom of the deck relative to the thickness of the deck. The results of their study showed that the drag coefficient becomes constant when the submergence ratio reaches a value between 4 and 5. Analysis of eq. [17] shows that, as the submergence ratio approaches a value of 5, the effects of submergence become negligible, which is similar to the finding of Malavasi and Guadagnini.

Figure 2*d* shows the variation of φ_4 with the Froude number Fr_1. The range of the parameter expressed by the measured data has been extended simply using the trend expressed by the data. As such, the power law fit to the data shown in the figure can be represented by

$$[18] \quad \varphi_4 = 1.1(1 - Fr_1)^{15} + 1.4$$

Fig. 3. Schematic illustration of the test setup used in the experiments.

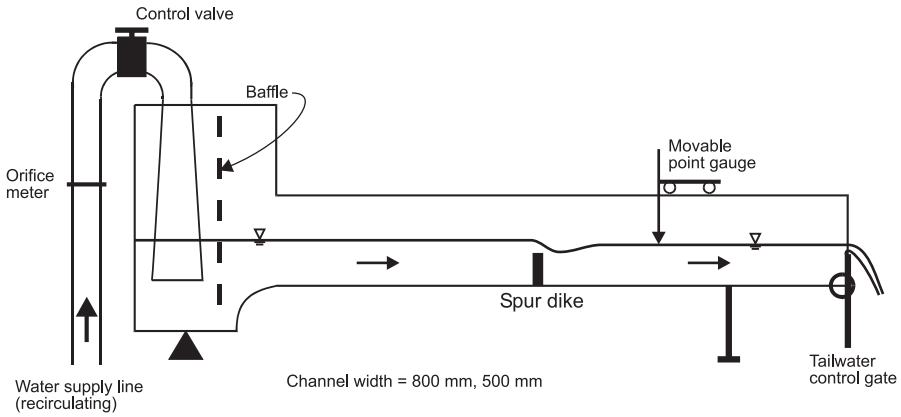

Here, it may be observed that, as with the other φ relationships, there is a decreasing trend with an increase in the influencing parameter, which in this case is the Froude number. The results of Ranga Raju et al. (1983) and Charbeneau and Holley (2001) on studies of bridge piers show the same trend. It may be noted that, in the present work as shown in Fig. 2*d* for Froude numbers greater than 0.2, the drag coefficient is constant.

4. Model validation and discussion

To provide for independent validation of the two spur dike backwater models described herein, a short series of tests was conducted in the Hydrotechnical Laboratory at the University of Saskatchewan. Two widths of flume were used in these tests to provide for a wider array of test conditions than those of the tests undertaken by Oak (1992). The test setup for both flumes is illustrated schematically in Fig. 3, and the test conditions are summarized in Table 2. Water surface levels were measured with a point gauge, and flow rates with an orifice meter and by a gravimetric method. A photograph showing the model spur dike in operation is shown in Fig. 4.

As part of this verification, reference was also made to the model of Oak and Smith (1994), which was also derived using Oak's (1992) data. It is referred to as the Oak and Smith model and can be expressed as

$$[19] \quad h_1/h_2 = 1 + 3.9(h_2/P)^{-2.4}(L/B)^{1.6}\, Fr_2^{1.5}$$

where Fr_2 is the Froude number of the flow downstream from the spur dike. Equation [19] was determined using regression analysis applied to Oak's submerged spur dike data (i.e., with overtopping). It can be used to solve for the upstream depth of flow, and hence the backwater effect, if the downstream flow conditions are known. Strictly speaking, it is only applicable over the range of conditions tested by Oak. The other two models are represented by eqs. [4] and [10] (i.e., the regression model) and eqs. [4] and [11] (i.e., the multiple function model).

The results of the validation tests are shown in Fig. 5. In each case, the backwater effect (i.e., $h_1 - h_2$) determined using each of the three models has been compared with that determined by experiment. The mean relative error calculated for each of the proposed multiple function model, the regression model, and the Oak and Smith model is 9.4%, 18.9%, and 42.0%, respectively. On the basis of these results, it is evident that the proposed multiple model provides the best estimate of the backwater effect due to the spur dike. It is to be realized, however, that the test conditions shown in Table 2 go beyond those represented by Oak's (1992) data. Thus, it is not necessarily reasonable to expect that the results from the regression model and the Oak and Smith model, which are based strictly on Oak's data, should yield a good prediction for test conditions outside the range of data from which they were developed. The proposed multiple function model, however, is specifically intended to represent a broader range of each test parameter.

Table 2. Range of experimental parameters used in the validation experiments.

Spur dike height, P (mm)	50
Spur dike length, L (mm)	200
Channel width, B (mm)	500, 800
Channel slope, S_o (m/m)	0
Downstream depth, h_2 (mm)	45–148
Downstream Froude number, Fr_2	0.22–0.88
Submergence ratio, h_1/P	1.22–3.02
Discharge, Q (L/s)	7.3–56.7

When the validation dataset is restricted to the range tested by Oak (1992), as shown in Table 1, the mean relative error calculated for each of the proposed multiple function model, the regression model, and the Oak and Smith model is 6.8%, 7.7%, and 24.3%, respectively. These results show that both the proposed multiple function model and the regression model more or less perform equally well in this instance. As well, both models perform considerably better than the Oak and Smith model, even when applied to the same data range used by Oak in his work.

It can be observed in Fig. 5 that the multiple function model provides better prediction of the backwater effect for lower backwater conditions (i.e., lower values of Δh). For higher values, the model slightly underestimates the actual backwater effect. One possible reason for the observed underestimate may be related to the determination of the effective tailwater depth in the model. It was observed during the validation tests that, for a particular discharge and tailgate setting, removal of the spur dike from the flow resulted in a change in the tailwater depth downstream from the spur dike

Fig. 4. Photograph showing the spur dike model in operation for one of the experiments.

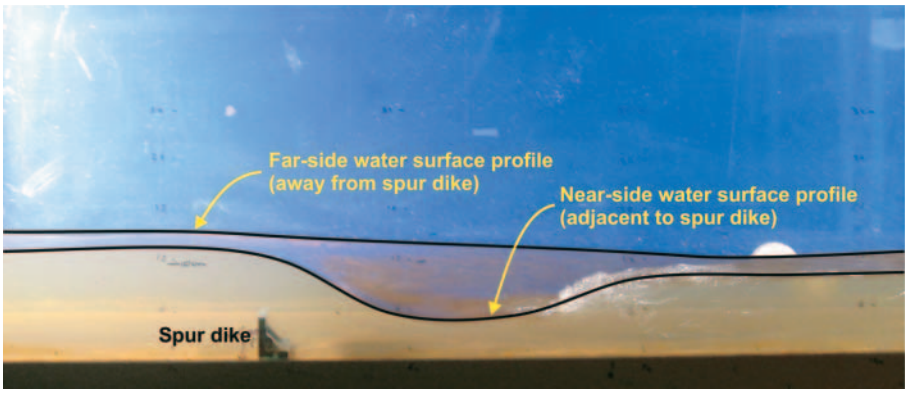

Fig. 5. Backwater prediction using (*a*) multiple function model; (*b*) regression model; and (*c*) Oak and Smith model. Calc., calculated; meas., measured.

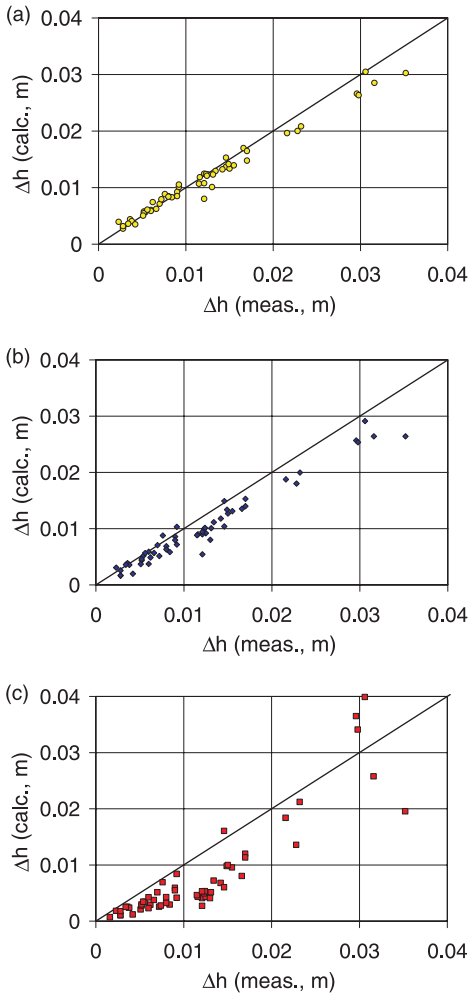

location. In particular, it was found that the downstream water level was higher with the spur dike removed than with the spur dike present. This difference persisted for the entire length of the flume, which in some respects is a bit confounding. Given the subcritical nature of the flow and the horizontal bed (i.e., zero slope), it is evident that the local effects due to the spur dike (i.e., impacts on flow depth and velocity) must have existed for the entire distance from the spur dike location to the end of the flume. The amount of water level adjustment became smaller as the tailwater depth increased, hence as the Froude number decreased, as one would expect given the smaller kinetic effects associated with lower Froude number flow conditions. Although the data do not exist to precisely quantify the magnitude of any error associated with determining the correct tailwater level, hence the backwater effect, the error is judged to be relatively small. Moreover, adjustment to the measured tailwater level would only serve to improve the apparent accuracy of the model predictions shown in Fig. 5.

Another possible source of error may be related to the assumption of a momentum correction factor of unity in eq. [1] (i.e., $\beta = 1$). Although a β value of unity may be approximately correct for the flow approaching the spur dike, it is likely that the factor is considerably greater than unity in the reach immediately downstream. The variation in the velocity distribution in the immediate downstream reach, both vertically and laterally, is expected to be considerable because of the complex flow conditions created by the spur dike. As it was not possible to measure the tailwater depth at a location far downstream from the spur dike where the β factor would have been nearer to unity, and as velocity distributions were not obtained as part of this study, the true momentum flux at the downstream section has invariably been underestimated. Nonetheless, if the downstream value of β were increased, it is evident from eq. [1] that, for a given value of drag coefficient (or drag force), the computed upstream depth and corresponding backwater effect would increase, which in turn would result in a better correlation between the predicated and measured backwater effects.

As a final comment, the results of this work may be extended to spur dikes with geometries other than that reported herein, such as spur dikes with a trapezoidal cross section as is usual in practice. Using a trapezoidal cross section with an attendant rounded nose, however, makes the structure more streamlined than is the case for a rectangular flat plate as used in this study. As such, determining the backwater effect using the results presented in this paper is likely to offer a somewhat conservative prediction (i.e., predicted backwater effect somewhat greater than that likely to occur). Until an improved predictive model is available for such situations, using the proposed model represents a safe approach.

5. Conclusions

The backwater effect due to a single spur dike in an open-channel flow was studied in a laboratory flume. Analysis of the flow regime was carried out using the momentum principle, with the resistance offered by the spur dike being expressed in terms of a drag coefficient. On the basis of a series of tests conducted by Oak (1992) and several validation tests conducted as part of this study, a so-called multiple function model has been proposed for predicting the drag coefficient, which in turn allows quantification of the backwater effect due to a single spur dike in the flow. In doing this work, it has been found that, as with other bluff bodies in an open-channel flow, the drag coefficient of a spur dike is a function of the structure geometry and flow condition, namely the spur dike aspect ratio, the contraction ratio, the submergence ratio, and the Froude number of the flow. It was also observed that the behavior of the parameters affecting the spur dike drag coefficient is similar to that for other bluff bodies.

The results of the study show that the submergence ratio has the greatest effect on the drag coefficient, especially for flow depths near to the spur dike height. The Froude number has the least effect on the drag coefficient. It was also found that the proposed multiple function model provides better backwater prediction capability than the other two models examined, particularly when a wide array of test conditions is evaluated. Furthermore, considering that a spur dike with a trapezoidal cross section is more streamlined than the two-dimensional spur dikes studied in this work (i.e., rectangular flat plates), backwater predictions made with the proposed multiple function model will be conservative.

Future work on this topic should address more specifically the nature of the backwater effect for three-dimensional spur dikes with a trapezoidal cross section and rounded nose. As well, work is needed on assessing the impact due to an array of spur dikes, such as that often used in various types of river training and bank protection works.

Acknowledgements

Financial support for this research has been provided by a University of Saskatchewan graduate scholarship to the first author and by funding from the Natural Sciences and Engineering Research Council of Canada through a grant to the second author. This support is gratefully acknowledged. The authors also thank the anonymous reviewers for their constructive comments on the initial version of the manuscript, all of which were useful in making for an improved final product.

References

Belz, J.U., Busch, N., Engel, H., and Gasber, G. 2001. Comparison of river training measures in the Rhine catchment and their effects on flood behavior. Water and Maritime Engineering, **148**(3): 123–132.

Charbeneau, R.J., and Holley, E.R. 2001. Backwater effects of piers in sub-critical flow. Technical Report FHWA/TX-0-1805-1, Texas Department of Transportation, Austin, Tex.

Criss, R.E., and Shock, E.L. 2001. Flood enhancement through flood control. Geology, **29**: 875–878.

Dalton, C.D., and Masch, D.F. 1968. Influence of secondary flow on drag force. ASCE Journal of the Engineering Mechanics Division, **94**(EM5): 1249–1257.

Hoerner, S.F. 1965. Fluid-dynamic drag: practical information on aerodynamic drag and hydrodynamic resistance. Hoerner Fluid Dynamics, Brick Town, N.J.

Malavasi, S., and Guadagnini, A. 2003. Hydrodynamic loading on river bridges. ASCE Journal of Hydraulic Engineering, **129**(11): 854–861.

Oak, A.G. 1992. Backwater rise due to a submerged spur. M.Sc. thesis, Department of Civil Engineering, University of Saskatchewan, Saskatoon, Sask. 68 pp.

Oak, A.G., and Smith, C.D. 1994. Backwater effect due to overtopping a spur dike. *In* Proceedings of the Annual Conference of the Canadian Society for Civil Engineering, Winnipeg, Man., 1–4 June 1994. Canadian Society for Civil Engineering (CSCE), Montréal, Que. Vol. 1, pp. 136–145.

Pinter, N. 2004. Technical review of the upper Mississippi River flow frequency study [online]. Southern Illinois University, Carbondale, Ill. Available from http://65.108.172.154/Issues/Floodplains/Rpt-PinterFinal.pdf) [accessed 29 June 2005].

Pinter, N., Thomas, R., and Wlosinski, J.H. 2001. Assessing flood hazard on dynamic rivers. EOS, Transactions of the American Geophysical Union, **82**(31): 333–339.

Ranga Raju, K.G., Rana, O.P.S., Asawa, G.L., and Pillai, A.S.N. 1983. Rational assessment of blockage effects in channel flow past smooth circular cylinders. Journal of Hydraulic Research, IAHR, **21**(4): 289–302.

Shaw, T.L. 1971. Effect of side walls on flow past bluff bodies. ASCE Journal of the Hydraulics Division, **97**(HY1): 65–79.

Shields, F.D. 1995. Fate of lower Mississippi river habitats associated with river training dikes. Aquatic Conservation: Marine and Freshwater Ecosystems, **5**(2): 97–108.

Soliman, M.M., Attia, K.M., Kotb, Talaat, A.M., and Ahmad, A.F. 1997. Spur dike effects on the river Nile morphology after High Aswan Dam. *In* Managing Water: Coping with Scarcity and Abundance, Proceedings of the 27th IAHR Congress, San Francisco, Calif., 10–15 August 1997. *Edited by* F.M. Holly, Jr., A. Alsaffar, and J.S. Gulliver. Thomas Telford, London, UK. Vol. A, pp. 805–810.

SPSS Inc. 1999. Statistical package for the social sciences. Version 9.0 [computer program]. SPSS Inc., Chicago, Ill.

Yossef, M.F.M. 2002. The effects of groynes on rivers (literature review). Delft Cluster Project 03.03.04, Delft University of Technology, Delft, The Netherlands. 51 pp.

List of symbols

a, b, c, d	exponents in regression equation
A_r	area ratio (= A_s/Bh_1)
A_s	upstream projected area of the spur dike (= PL)
B	width of flume
C_D	drag coefficient due to spur dike
C_{Do}	drag coefficient corresponding to free-stream conditions
D	pier diameter
F_1	force due to upstream hydrostatic pressure distribution
F_2	force due to downstream hydrostatic pressure distribution
F_D	drag force due to spur dike
F_f	friction force due to boundary friction
Fr_1	Froude number upstream of spur dike (= $V_1/(gh_1)^{1/2}$)
Fr_2	Froude number downstream from spur dike (= $V_2/(gh_2)^{1/2}$)
g	acceleration due to gravity (i.e., 9.81 m^2/s)

h_1 depth of flow upstream of spur dike
h_2 depth of flow downstream of spur dike
K constant in regression analysis
L length of spur dike
P height of spur dike
q unit discharge (= Q/B)
Q volumetric discharge
R^2 square of the correlation coefficient
Re_1 Reynolds number upstream of spur dike
S_o channel slope
V representative velocity
V_1 average velocity upstream of spur dike
V_2 average velocity downstream from spur dike
α angle between spur dike and stream bank
β momentum correction factor
β_1 momentum correction factor upstream of spur dike
β_2 momentum correction factor downstream from spur dike
Δ spur dike shape factor
Δh backwater effect due to spur dike ($h_1 - h_2$)
ρ fluid density
φ_1 drag coefficient expressed in terms of aspect ratio
φ_2 drag coefficient expressed in terms of opening ratio
φ_3 drag coefficient expressed in terms of submergence ratio
φ_4 drag coefficient expressed in terms of Froude number